RSC Advances

PAPER

View Article Online
View Journal | View Issue

Cite this: *RSC Adv.*, 2019, **9**, 8350

Flexible cupric oxide photocathode with enhanced stability for renewable hydrogen energy production from solar water splitting†

Yang Li *[abc] and Kai Luo[a]

CuO is a promising but unstable photocathode in solar water splitting. Herein, a flexible CuO photocathode is prepared and its degradation mechanisms and stabilization strategies have been discussed. Briefly, we find alkali environment and low light intensity are the critical factors in the stabilization of the CuO photocathode. For practical usage, a composite semiconductor layer, composed of TiO_2, La_2O_3 and NiO, is deposited on the CuO photocathode, which is proved to be effective for enhancing the stabilization of the CuO photocathode. 100% of the photocurrent density has been retained after 20 minutes of continuous illumination. The optimized stable photocurrent density is measured as 0.3 mA cm^{-2} at 0.5 V_{RHE}.

Received 1st February 2019
Accepted 4th March 2019

DOI: 10.1039/c9ra00865a

rsc.li/rsc-advances

The lack of suitable photocathode materials for water reduction seriously limits the development of solar water splitting.[1,2] Cupric oxide (CuO) is an attractive cathode candidate for photoelectrochemical (PEC) water splitting due to its narrow band gap (1.44–1.68 eV), low cost, and nontoxicity.[3] Nonetheless, the enormous potential of the CuO photocathode has not received enough attention probably because the conduction band was considered to be more positive than the potential of the water reduction reaction (0 V *versus* NHE, Normal Hydrogen Electrode) from the theoretical calculation, and unfavorable for hydrogen production.[4] More seriously, copper-based oxides, including CuO and Cu_2O, suffer from fast photo-induced corrosion, whose stabilities are far from those of the typical photoanodes, such as WO_3 and α-Fe_2O_3.[5,6] For decades, scientists dreamt of stabilizing the CuO photocathode in aqueous electrolytes at comparatively low potentials, especially at 0 V_{RHE} (RHE = Reversible Hydrogen Electrode), and there are few successful cases.[1] The direct reason is probably the unsolved degradation mechanism and the complex side effects of CuO photocathode in the water splitting reaction. Herein, we report a facile and highly effective low-cost strategy based on synthesizing flexible CuO photocathode, followed with the analyses of the influence of electrolyte environment, bias potential and light intensity on CuO photocathode stability, at last we designed a multiple overlayer, which takes into consideration of advantages of each individual layer. The optimized CuO shows remarkably enhanced photo-stability with 100% retention of the photocurrent density after 20 min.

From the SEM images in Fig. 1a, we can see the pre-clean Cu foil exposed a comparatively smooth morphology. After a fast fire treatment, a dense and brunette oxide layer grew on the metal surface. The oxide layer thickness increases as the fire treatment period extends. The average film thickness is 150 nm after 10 s of the fire treatment confirmed by the cross section SEM images, which is much thinner in comparison with the

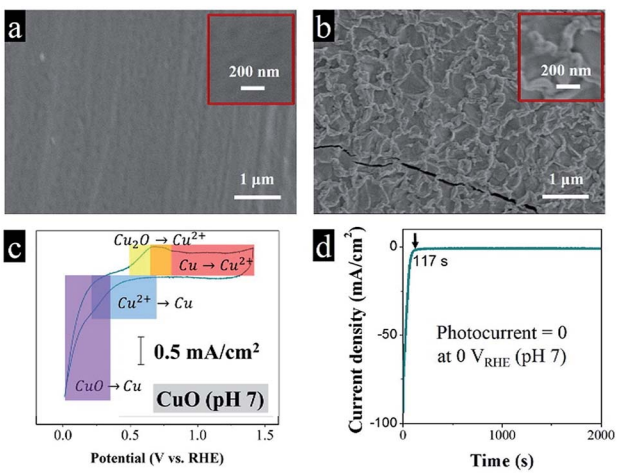

Fig. 1 SEM images of (a) the Cu foil and (b) the CuO photocathode, respectively; (c) cyclic voltammetry of the CuO photocathode in 1 M $NaSO_4$ electrolyte (pH 7); (d) dark current density of the CuO photocathode at 0 V_{RHE} in pH 7 without any photoresponse.

[a]*School of Energy and Power, Jiangsu University of Science and Technology, Zhenjiang, Jiangsu, 212003, P. R. China. E-mail: yang_li@just.edu.cn*

[b]*School of Science, Tianjin University, Tianjin, 300072, China*

[c]*Collaborative Innovation Center of Chemical Science and Engineering (Tianjin), Tianjin Key Laboratory of Applied Catalysis Science and Technology, State Key Laboratory of Chemical Engineering, School of Chemical Engineering, Tianjin University, Tianjin, 300072, China*

† Electronic supplementary information (ESI) available. See DOI: 10.1039/c9ra00865a

traditional calcination in a muffle furnace.[7] The moderate thickness is convenient for the separation of charge carriers, preventing fast recombination.[8] The metal interlayer serves to transfer electrons, while the oxide layer is responsible for absorbing photons and generating free electrons. Fig. 1b implies the fast fire treatment caused thermal expansion and contraction, produced a rough and wrinkled oxide layer.

It is a common that acidic electrolytes benefit hydrogen evolution reaction, because of high concentrations of protons.[9] In previous studies, most of the colleagues try their best to improve the performance of CuO photocathode in Na_2SO_4 electrolyte.[10,11] However, the cyclic voltammetry in Fig. 1c demonstrates that $Cu^{(2+)}O$ spontaneously corrupts to $Cu^{(0)}$ below 0.3 V_{RHE} (eqn (1)), which is buttressed by our photoelectrochemical test in Fig. 1d, predictably, the CuO photocathode deactivated abruptly in dark (the dark current density reached 93 mA cm^{-2} at 0 V_{RHE}), and totally no photocurrent can be observed under illumination (the dark current density decayed to a stable value of 0.5 mA cm^{-2}). After the reaction, the brunette absorbing layer disappeared, recovered a shiny metallic luster.

$$CuO + 2e^- + 2H^+ \rightarrow Cu + H_2O,\ E^\theta = +0.3\ V_{RHE} \quad (1)$$

To avoid the fast self-corrosion of the CuO photocathode below 0.3 V_{RHE}, at the same time for the further combination with the photoanodes, we increased the voltage applied to CuO photocathode to 0.5 V_{RHE}, and at this time we found a photocurrent spike of 0.8 mA cm^{-2} appeared, followed by a continuous decrease to 0.1 mA cm^{-2} after 1000 s irradiation in Fig. 2a. The result implies that a slow deactivation process still exists, similar to the phenomenon in Jang's work.[3] In the retardatory deactivation process, the surface $Cu^{(2+)}O$ is reduced to $Cu^{(0)}$, eqn (1), by the energetic photo-induced electrons. The accumulated Cu layer isolates the inner CuO from the electrolyte, which slows down the current decay. The extreme instability of CuO photocathode forced us to find a new path of using it.

After realizing that CuO is extremely sensitive to protons, which causes fast photo-induced inactivation, we tried to raise the pH value and reduce the proton concentration. Adjusting pH value is often an effective means for changing the course of a chemical reaction.[12,13] After substituting NaOH for Na_2SO_4 in the electrolyte, we discovered that the CuO photocathode produced a photocurrent density of 1.2 mA cm^{-2} at 0.5 V_{RHE} in pH 13 without any decay during 1000 s. It is meaningful to find adjusting pH value has an ability to alter the selectivity of the CuO photocathode, which seems the easiest way to stabilize the CuO photocathode. As shown in Fig. 2b, according to the previous studies, the Fermi level of CuO is near to 0.8 V_{RHE}, while the calculated band gap is 1.6 eV.[3,14] As CuO is a p-type semiconductor, assuming that the energy gap between Fermi level and valence band is 0.3 eV,[15,16] the conduction band and valence band are −0.5 V_{RHE} and 1.1 V_{RHE}, respectively. Consequently, in the neutral condition, photo-excited electrons in the conduction band move downward and reduce surface CuO to Cu. As a result, we observed a fast descent of the photocurrent density. As mentioned above, the accumulated Cu layer isolates

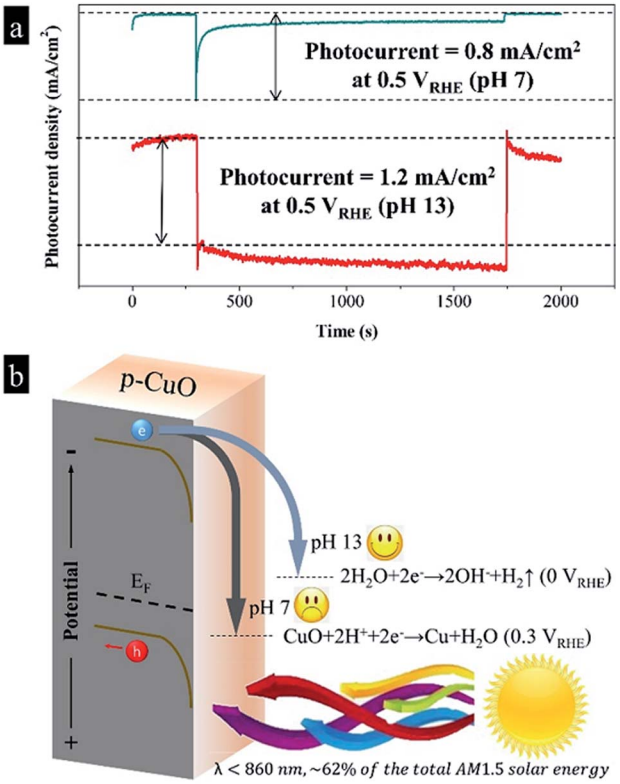

Fig. 2 (a) The photoelectrochemical stabilities of the CuO photocathodes in 1 M Na_2SO_4 (pH 7) and 1 M NaOH (pH 13) electrolytes at 0.5 V_{RHE}, respectively; (b) schematic plot of the band structure and photodeactivation mechanism of the CuO photocathode.

the inner CuO from the electrolyte, which slows down the current decay. Comparatively, photo-induced electrons selectively reduce water into hydrogen in the basic environment, while the deactivation reaction is somewhat neglected. The least of perfection, in the basic solution the good stability was accompanied by a slow recovery of the dark current.[4]

$$CuO + H_2O + 2e^- \rightarrow Cu + 2OH^-,\ E^\theta = +0.3\ V_{RHE} \quad (2)$$

After tuning the light intensity from 100 mW cm^{-2} to 20 mW cm^{-2}, it is really interesting to find the relaxation of dark current disappeared, although the photocurrent density decreased to 0.3 mA cm^{-2}. It is not difficult to associate this relationship with the shift of Fermi level. We interpret the mechanism in Fig. 3, under the powerful beam, the Fermi level transfers to the potential that is higher than the E^θ(Cu/CuO), in this case, the photo-excited electrons partially reduce surface CuO to Cu (eqn (2)), followed by generating $Cu(OH)_2$ spontaneously (eqn (3)). $Cu(OH)_2$ is a weak p-type semiconductor, leading to the relaxation phenomenon. Oppositely, the Fermi level stays below the E^θ(Cu/CuO) under low light intensity, which inspires the photo-electrons to fulfill the water reduction. Consequently, CuO photocathode shows a satisfactory photostability at 0.5 V_{RHE} with 100% retention of the photocurrent density after 20 min.

$$Cu + 2OH^- + 2h^+ \rightarrow Cu(OH)_2,\ E^\theta = -0.2\ V_{RHE} \quad (3)$$

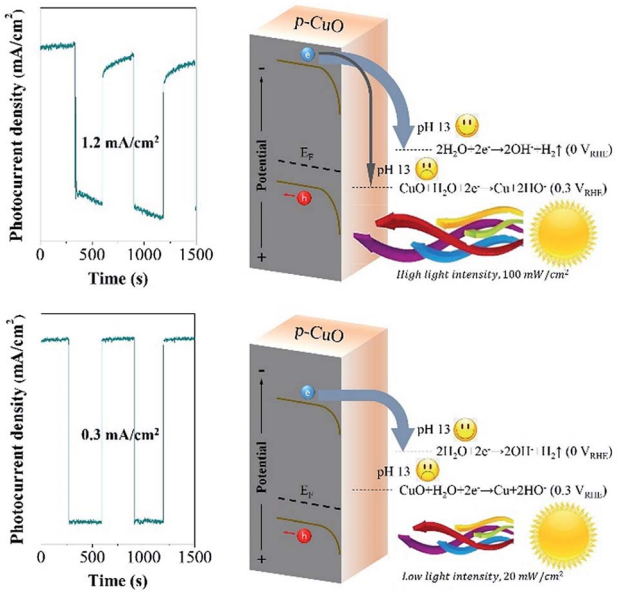

Fig. 3 The comparison of the mechanism at pH 13 under high light intensity (100 mW cm^{-2}) and low light intensity (20 mW cm^{-2}).

As known to all, the power of sunlight varies with time in real life, it is really difficult to limit the maximum value from 100 mW cm^{-2} to 20 mW cm^{-2}. Afterwards, we designed a triple-component protective layer of $TiO_2/La_2O_3/NiO$ to neutralize the disadvantage, the thicknesses of TiO_2, La_2O_3 and NiO were 50 nm, 100 nm and 18 nm, respectively. The different film thicknesses were obtained by controlling the dip-coating processes (ESI†). The multilayer structure not only controls the light intensity within an appropriate range but also has a catalytic influence. The TiO_2 wrapped the CuO surface and reduced the surface roughness in Fig. 4a, while the subsequent La_2O_3/NiO totally covered the substrate, making the surface smooth under the electron microscope (Fig. 4b). The optimized CuO photocathode (Fig. 4c) produced a thoroughly stable photocurrent density of 0.3 mA cm^{-2} at 0.5 V_{RHE} under AM 1.5 G condition for 20 min, meanwhile, the dark current density recovers quickly and keeps steady, shown in Fig. 5a.

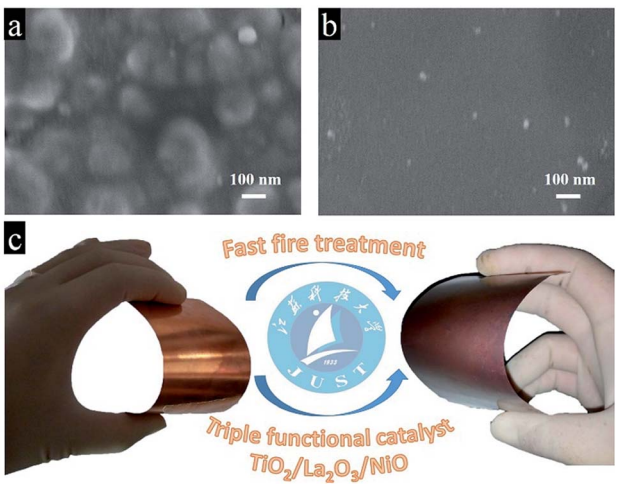

Fig. 4 The surface SEM images of (a) the CuO/TiO_2 and (b) the CuO/TiO_2/La_2O_3/NiO; (c) schematic plot of the preparation of the CuO/TiO_2/La_2O_3/NiO photocathode.

The high stability of around 100% is found to be the highest reported value in terms of a plain CuO photocathode (Table 1). To certify the fundamental chemical stability, X-ray photoelectron spectroscopy (XPS) was applied to detect the surface properties and oxidation states, shown in Fig. 5b. X-ray induced Auger electron spectroscopy (XAES) was employed in the Cu LMM region to get information of the oxidation state of Cu (Fig. 5b), as the Cu 2p binding energies are almost indistinguishable. The Cu LMM peak at 917.7 eV was assigned to Cu^{2+}. The binding energies of Ti $2p_{3/2}$, La $3d_{5/2}$ and Ni $2p_{3/2}$ were 458.7, 834.5 and 835.7 eV, respectively, corresponding to $Ti^{(4+)}$, $La^{(3+)}$ and $Ni^{(2+)}$. Furthermore, the XPS spectra before and after reactions in Fig. S1† indicate the metal oxidation states in $Cu^{(2+)}O$, $Ti^{(4+)}O_2$, $La^{(3+)}{}_2O_3$ and $Ni^{(2+)}O$ did not change after 30 min reaction, which met our expectations. Moreover, the construction of this multi-layer photocathode is depicted in Fig. 5c. Many researchers predicted that the conduction band position of CuO is not negative enough to drive the hydrogen evolution reaction. In fact, we found CuO possesses a conduction band edge near to −0.5 V_{RHE}, which means the photoelectrocatalytic hydrogen evolution from water by CuO should be thermodynamically favorable. In the present work, the photo-induced electrons in p-CuO were driven by the depletion layer (p-CuO/n-TiO_2 p–n junction) to n-TiO_2, then penetrated the La_2O_3 layer. Herein, La_2O_3 can be considered as a proton insulating layer.[17] After hundreds of attempts, we found that La_2O_3 is one of the materials that effective for the stabilization

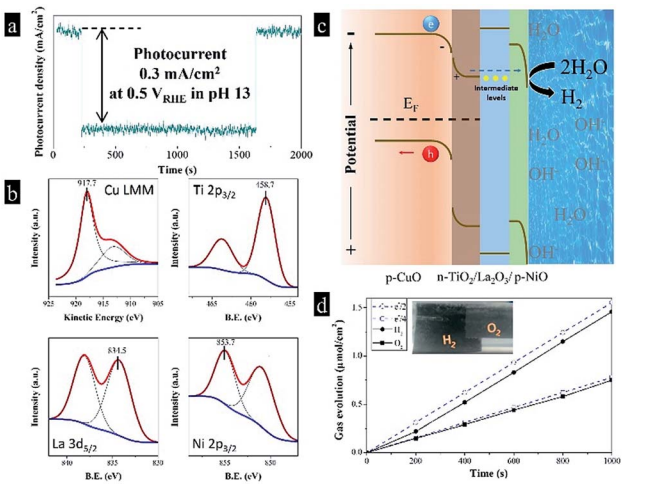

Fig. 5 (a) Photoelectrochemical response and stability of the TiO_2/La_2O_3/NiO coated CuO photocathode; (b) Cu LMM, Ti 2p, La 3d and Ni 2p X-ray photoelectron spectra (XPS) of the TiO_2/La_2O_3/NiO coated CuO photocathode; (c) schematic plot of the band structure and water reduction mechanism of the TiO_2/La_2O_3/NiO coated CuO photocathode; (d) gas evolution from the CuO/TiO_2/La_2O_3/NiO photocathode and the Pt counter electrode, which is compared with the evolution of H_2 ($e^-/2$) and O_2 ($e^-/4$) expected from the photocurrent. The measurement was performed at constant potential 0.5 V *vs.* RHE.

Table 1 The stabilities of the CuO photocathodes for PEC water splitting in the literature

Electrolyte	Light intensity (mW cm^{-2})	Bias (V_{RHE})	Constructure	Stability	Ref.
0.25 M Na_2SO_4	109	0	ZnO/CuO	40% (3 min)	21
1 M NaOH	100	0.25	CuO	40% (20 min)	22
0.5 M Na_2SO_4	100	0.2	CuO	80% (15 min)	3
0.25 M Na_2SO_4	100	0.2	ZnO/CuO	90% (6 min)	23
0.5 M Na_2SO_4	100	0	Au–Pd/CuO	90% (20 min)	24
0.1 M Na_2SO_4	100	0.2	CuO	70% (15 min)	25
0.1 M Na_2SO_4	100	0.05	CuO	90% (5 min)	10
1 M NaOH	100	0.5	CuO	~100% (20 min)	Present work

of copper oxide, and the stability enhanced with the increasing thickness, until a thickness of 100 nm can balance the stability and the activity. Although La_2O_3 has a large theoretical band gap (3.8–5.8 eV), it contains deep levels and trap-states, which reduce the band gap (2.9 eV, fluorescence emission at 416 nm) and the resistivity (~10 kΩ cm).[18–20] The deep levels and trap-states form intermediate levels in the large band gap, facilitating the charge transportation. Thus, La_2O_3 accepts the photo-induced electrons from TiO_2 and allow them to pass through. Finally, the electrons enter a second depletion layer, as p-NiO equilibrates with the electrolyte, and complete the water reduction. By the way, we have to mention that TiO_2, La_2O_3 and NiO perform their respective duties and are indispensable. The amounts of H_2 and O_2 that evolved were determined by gas chromatography. In Fig. 5d, the theoretical amounts of gases expected from photocurrent generations are compared with the actual generation of the gases. The difference between these two values is represented by the faradaic efficiency. The faradaic efficiency of the hydrogen evolution was determined to be 94% when the system was stabilized and showed a steady state. The rest 6% could be accounted for the inefficient gas collection (gas dissolution and strong adsorption on the electrode surface) and some parasitic electrochemical processes.

Conclusions

Cupric oxide is not chemically inert in aqueous solution under illumination because of its sensitivity to protons, which makes a painstaking process of fabricating stable CuO photocathodes. It is found the photo-stability of CuO photocathode is highly dependent on the pH value, working potential, light intensity and protective overlayer. After optimization, we applied CuO photocathode in basic environment coupled with a multifunctional semiconductor overlayer, *i.e.* $TiO_2/La_2O_3/NiO$, in which p-CuO/n-TiO_2 forms a p–n junction, accelerating the charge separation, while La_2O_3 and NiO act as a proton-isolating layer and a catalyst layer, respectively. The photocurrent density is 0.3 mA cm^{-2} at 0.5 V_{RHE} with 100% retention after 20 min, as well as the dark current density.

Conflicts of interest

There are no conflicts to declare.

Acknowledgements

This work has been supported by National Nature Science Foundation of China (No. 21606171), China Postdoctoral Science Foundation (No. 2015M580205 and 2017T100160), and Tianjin University Independent Innovation Foundation (1705).

Notes and references

1 M. G. Walter, E. L. Warren, J. R. McKone, S. W. Boettcher, Q. Mi, E. A. Santori and N. S. Lewis, *Chem. Rev.*, 2010, **110**, 6446–6473.
2 K. Sivula, *Chimia*, 2013, **67**, 155–161.
3 Y. J. Jang, J. W. Jang, S. H. Choi, J. Y. Kim, J. H. Kim, D. H. Youn, W. Y. Kim, S. Han and J. Sung Lee, *Nanoscale*, 2015, **7**, 7624–7631.
4 X. B. Chen, S. H. Shen, L. J. Guo and S. S. Mao, *Chem. Rev.*, 2010, **110**, 6503–6570.
5 Y. Li and H. Chen, *J. Mater. Chem. A*, 2016, **4**, 14974–14977.
6 Y. Li, N. Guijarro, X. Zhang, M. S. Prevot, X. A. Jeanbourquin, K. Sivula and H. Chen, *ACS Appl. Mater. Interfaces*, 2015, **7**, 16999–17007.
7 Y. Li, X. Zhang, H. Chen and Y. Li, *Catal. Commun.*, 2015, **66**, 1–5.
8 Y. Li, Z. Yu, J. Meng and Y. Li, *Int. J. Hydrogen Energy*, 2013, **38**, 3898–3904.
9 S. Trasatti, *J. Electroanal. Chem. Interfacial Electrochem.*, 1972, **39**, 163–184.
10 Y. F. Lim, C. S. Chua, C. J. Lee and D. Chi, *Phys. Chem. Chem. Phys.*, 2014, **16**, 25928–25934.
11 Z. Yu, J. Meng, Y. Li and Y. Li, *Int. J. Hydrogen Energy*, 2013, **38**, 16649–16655.
12 S. Štrbac and R. R. Adžić, *Electrochim. Acta*, 1996, **41**, 2903–2908.
13 S. Yasutomi, T. Morita and S. Kimura, *J. Am. Chem. Soc.*, 2005, **127**, 14564–14565.
14 Q. Huang, F. Kang, H. Liu, Q. Li and X. Xiao, *J. Mater. Chem. A*, 2013, **1**, 2418–2425.
15 Y. Matsumoto, *J. Solid State Chem.*, 1996, **126**, 227–234.
16 Y. Li, X. Zhang, S. Jiang and Y. Li, *J. Catal.*, 2014, **320**, 208–214.
17 D. Bae, B. Seger, P. C. K. Vesborg, O. Hansen and I. Chorkendorff, *Chem. Soc. Rev.*, 2017, **46**, 1933–1954.

18 G. Shang, P. W. Peacock and J. Robertson, *Appl. Phys. Lett.*, 2004, **84**, 106–108.
19 C. G. Hu, H. Liu, W. T. Dong, Y. Y. Zhang, G. Bao, C. S. Lao and Z. L. Wang, *Adv. Mater.*, 2007, **19**, 470–474.
20 S. S. Kale, K. R. Jadhav, P. S. Patil, T. P. Gujar and C. D. Lokhande, *Mater. Lett.*, 2005, **59**, 3007–3009.
21 A. Kargar, Y. Jing, S. J. Kim, C. T. Riley, X. Pan and D. Wang, *ACS Nano*, 2013, **7**, 11112–11120.
22 M. Patel, R. Pati, P. Marathey, J. Kim, I. Mukhopadhyay and A. Ray, *J. Electrochem. Soc.*, 2016, **163**, H1195–H1203.
23 F. Wu, F. Cao, Q. Liu, H. Lu and L. Li, *Sci. China Mater.*, 2016, **59**, 825–832.
24 S. Masudy-Panah, R. Siavash Moakhar, C. S. Chua, A. Kushwaha and G. K. Dalapati, *ACS Appl. Mater. Interfaces*, 2017, **9**, 27596–27606.
25 J. Han, X. Zong, X. Zhou and C. Li, *RSC Adv.*, 2015, **5**, 10790–10794.